International Journal of Heat and Fluid Flow 29 (2008) 1411–1421

Contents lists available at ScienceDirect

International Journal of Heat and Fluid Flow

journal homepage: www.elsevier.com/locate/ijhff

Multi-scale analysis of hydrodynamics inside a network of crossing minichannels using electrodiffusion method and PIV measurements

F. Huchet [a], J. Comiti [a], P. Legentilhomme [a], C. Solliec [b], J. Legrand [a,*], A. Montillet [a]

[a] GEPEA, Université de Nantes, CNRS, UMR 6144, C.R.T.T, 37 Bd de l'université, BP 406, 44602 Saint-Nazaire-Cedex, France
[b] GEPEA, Université de Nantes, CNRS, UMR 6144, Ecole des Mines de Nantes, 4, rue A. Kastler, 44307 Nantes Cedex 3, France

ARTICLE INFO

Article history:
Received 11 July 2007
Received in revised form 24 April 2008
Accepted 29 April 2008
Available online 20 June 2008

Keywords:
Crossing minichannels
Network
Electrochemical method
Particle image velocimetry
Wall turbulence scales
Intermittency
Statistic turbulence properties

ABSTRACT

Knowledge of local hydrodynamics inside miniaturized systems is necessary for industrial applications. In this work two techniques are used in order to characterize the flow in a network of crossing minichannels. These techniques are respectively based on the particle image velocimetry and on electrochemical microsensors used in the local diagnostic of the flow in order to set-up multi-scale analysis of the hydrodynamics inside a tested system. PIV measurements are applied in front of electrochemical sensors in order to obtain mean velocity fields along the cell. The comparison of velocity profiles with that obtained in fully developed channel flow emphasize the developing behaviour of the flow between two successive crossings. Vortices in the near wall region have been detected using the electrochemical technique at different positions corresponding to the location of the electrodes. The calculation of statistic parameters such as flatness and skewness factors of the instantaneous values of wall shear rate shows that the flow exhibits an intermittent regime behaviour. Finally, a multi-scale hydrodynamics pattern is proposed to describe the turbulence properties in the near wall region at the crossing of two channels.

1. Introduction

Microfluidic systems investigation presents an important challenge for researchers because it gives rise to the development of various micro-devices such as micro-pumps, micro-valves, microchannel heat sinks for electronic devices and microreactors in chemical processes, among a wide range of applications. An understanding of transfer phenomena, such as local hydrodynamics, is crucial for industrial applications. The miniaturization of industrial equipment such as mixers, reactors or heat and mass exchangers represents an innovation in process engineering (Gavrilidis et al., 2002).

Especially in microfluidic devices, the increase of the ratio between the transfer surface area and the fluid volume gives rise to enhanced heat and mass transfer. Many works dealing with mixing in various geometries of microchannels were dedicated to the investigation of these new tools of production involved in chemical and biological transformations (Kockmann et al., 2006; Hansen and Quake, 2003).

A characterization of the flow behaviour and of heat and mass transfer performance is needed in order to develop and improve these microsystems for their application in process engineering. A large number of studies dealing with flow through microsystems of different shapes and flow configurations is available in the literature since a few years. Among them, T-microchannel (Bothe et al., 2006) or hydrodynamics focusing (Wu and Nguyen, 2005) are some promising classes of flow configurations for micro-mixer applications. Various complex geometries are usually studied by using numerical approaches or global measurements to characterize transfer phenomena in heat exchangers (Brandner et al., 2006) or microreactors (Commenge et al., 2004). The flow inside these microreactors or microexhangers are usually in the transitional or turbulent regime and the experimental description of all the hydrodynamics scales become more difficult than in classical macrodevices. In the mixing research area, the characterization of the mixing scales is nevertheless fundamental for the design and the optimization of the microscale devices. The fluid flow at the microscale level is mainly connected to the characteristics of flow in the transitional and turbulent regimes. The conditions of stationarity, homogeneity and isotropy cannot be assumed in confined turbulent flow in microsystems. Thus, it is of some importance, from both academic and practical points of view, to study confined flow and mixing with particular attention given to the small scale motion. In spite of the recent work dealing with local hydrodynamics analysis inside microchannels, in particular by μPIV (Li and Olsen, 2006), very few works are dedicated to both hydrodynamics and mixing at the small scales especially in the near wall vicinity. A high sampling frequency is required to adequately describe a confined turbulent flow characterized by non-Gaussian and high level

* Corresponding author. Tel.:+33 240172633; fax: +33 240172618.
E-mail address: jack.legrand@gepea.univ-nantes.fr (J. Legrand).

0142-727X/$ - see front matter © 2008 Elsevier Inc. All rights reserved.
doi:10.1016/j.ijheatfluidflow.2008.04.012

Nomenclature

A	surface area of the microelectrode, m^2
c_0	bulk concentration, mol m^{-3}
D	diffusion coefficient, $m^2\ s^{-1}$
d_e	diameter of circular probes, m
d_h	hydraulic diameter, m
F	flatness factor of the wall shear rate, $\langle s'^4\rangle/\langle s'^2\rangle^2$
H	length of the cell, m
$I_{\lim}(t)$	limiting diffusion current, A
$\bar{I}_{\lim}$	mean diffusion limiting current, A
IT	dimensionless second-order moment of the velocity
k	mass transfer coefficient, $m\ s^{-1}$
L	width of the cell, m
Re	Reynolds number
R^*_{ss}	dimensionless autocorrelation
$s(t)$	instantaneous wall shear rate, s^{-1}
$\bar{s}$	mean wall shear rate, s^{-1}
s'	fluctuating wall shear rate, s^{-1}
S_k	skewness factor of the wall shear rate, $\langle s'^3\rangle/\langle s'^2\rangle^{3/2}$
s_q	quasi-steady solution of wall shear rate, s^{-1}
t_0	characteristic time probe, s
U	velocity measured by PIV, $m\ s^{-1}$
U_c	individual minichannel velocity, $m\ s^{-1}$
X/H	dimensionless axial length of the cell

Greek symbols

δ_d	mass boundary layer thickness, m
$\Im$	Faraday's constant, C
λ	Taylor microscale, m
Λ	integral macroscale, m
v_e	number of electrons involved in redox reaction
ν	kinematic viscosity, $m^2\ s^{-1}$

fluctuations. Recently, it constitutes an important challenge for classical turbulence investigations techniques. (Natrajan and Christensen, 2007; Natrajan et al., 2007).

In our study, we propose to characterize the local hydrodynamics inside a network of crossing minichannels intersecting at right angles. The cell is a geometric model to study a complex confined flow such as those met in certain mini-heat-exchangers or mini-catalytic-reactors. Two methods of flow investigation were used, in particular an electrochemical method allowing investigation of the near wall turbulence. The two complementary approaches are:

- PIV measurements in order to obtain flow map and especially mean velocity fields inside the network of crossing minichannels,
- the electrochemical method that allows to measure turbulent quantities in the viscous sub-layer at different locations in the minichannels.

The electrochemical method using small probes has been first and widely used to obtain the local wall shear rate. The application of this technique to turbulence investigation was initiated by Reiss and Hanratty (1963) and further developed by, in particular, Lebouché (1968), Deslouis et al. (1990), Sobolik et al. (1998) or Legrand et al. (1997).

Preliminary works on the present geometry performed by Huchet et al. (2007) found similar results to those in porous media, especially regarding the flow regime (Seguin et al., 1998a,b). The flow is found to be laminar and the pressure drop governed by viscous dissipation only at low Reynolds number ($Re < 10$). For $Re > 10$ the flow regime remains laminar but the pressure drop is described by a Forcheimer type equation due to the kinetic energy degradation. Shear rate fluctuations are observed for $Re > 200$. Under transitional flow conditions, the fluctuation rate increases rapidly and reaches a locally constant level above a Reynolds number of about 1000. Moreover, Huchet et al. (2007) performed measurements of global mass transfer and confirm that the network of crossing minichannels can rather be compared to a porous media than to set of straight channels.

In the present paper, the near wall flow analysis by electrochemical method coupled with the whole hydrodynamic behaviour obtained by PIV (Section 3) gives a fine-scale description of the flow characteristics. An order of magnitude of the real size of the liquid eddies responsible of the mixing at the small scales (Section 4.1) has been calculated. We investigate the wall shear rate fluctuations (Section 4.2) which are linked to the scalar field fluctuations of the electrochemical species (here, ferri-ferrocyanide). The skewness and flatness factors were used to investigate the mixing characterization in the near vicinity of the wall (in terms of anisotropy and intermittency) along the network. This approach allows, without using semi empirical hypotheses, to link the statistical characteristics of turbulent mass transfer (turbulent mass flux, statistical characteristic of current fluctuations) to the statistical characteristics of near wall turbulence. Conclusions (Section 5) are finally drawn.

2. Materials and method

2.1. Experimental cell

The experimental cell is shown in Fig. 1. It was made of two altuglas plates and features crossing minichannels in the upper plate. The individual square-cross sections of the channels (1.5 mm in side) intersected at right angles. The whole test section had a length of $H = 105$ mm and a width of $L = 52$ mm. A calming

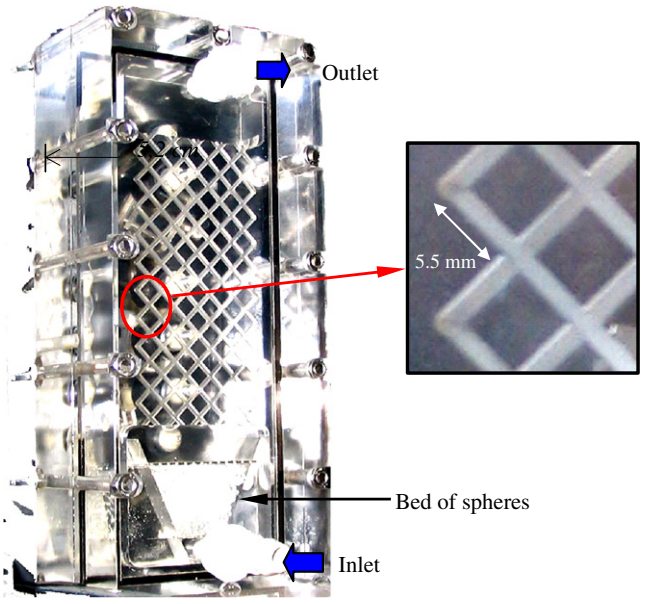

Fig. 1. Experimental cell with square-cross sections of the minichannels: (1.5 mm × 1.5 mm).

section containing glass spheres 2 mm in diameter, allowed a better distribution of the fluid in the ten minichannels inlets of the network.

Two bottom plates were successively used in order to perform the two measurements techniques. One includes 39 circular platinum microelectrodes flush-mounted to the wall allowing an electrodiffusion diagnostics of the wall flow. The second one is a transparent plate required for the visualization in the frame of PIV measurements.

2.2. Description of the PIV apparatus

The experimental testing bench included a laser (Nd-Yag, 15 Hz, 120 mJ), a double image recorder camera (Kodak megaplus ES 1.0, 1008 × 1016 pixels) which was joined to a 28 mm lens and three macroscopic sleeves. The dedicated processor (PIV 2100) and Flowmanager V 4.5 software were used to perform the calculations of the flow fields using the cross-correlation method. The seeding material was spherical polyamide particles from Dantec (density = 1.03, d_p = 20 μm). Interrogation areas were squares of 32 × 32 pixels. The laser, the CCD camera and the cell were placed on an individual moving system. The water pump was preceded by a mixer and the working cell was placed on a stiff table mounted on slender screws in order to reduce the vibrations induced by the pump. Micrometric moving systems were used to align the laser beam in the fluid plane and to accurately focalize the camera on the measurement plane. By moving the laser, the thickness of the laser sheet crossing the network cell had a minimum value less than 1 mm.

In those conditions, the magnification ratio was closed to 1:1 and the investigated visualization field measured was 1 cm × 1 cm. The field depth of the image was measured by a diffraction grating and was approximately equal to 300 μm. The seeding concentration was adjusted to get between 5 and 10 particles in each interrogation window. The statistical averaging of the data was performed on a series of 1000 instantaneous velocity fields and the statistical convergence was checked on mean velocity, $\overline{U}$, and second-order moments of fluctuating velocity.

The measurements were focused on eight zones corresponding to the location of the electrochemical probes. The experiments were performed at Reynolds number, *Re*, ranged from 145 to 1620. *Re* is based on the mean channel velocity inside individual channel, U_c, and the hydraulic channel diameter, d_h:

$$Re = U_c d_h / \nu, \tag{1}$$

where ν is the kinematic viscosity of the working fluid. In this paper, the presented results are limited to three zones (Fig. 2) along the network were chosen to present the PIV results. These ones (zone 1 at the inlet, zone 2 in the middle and zone 3 at the outlet of the network) reveal all of characteristics of the flow observed inside the network.

2.3. Electrodiffusion technique

The electrodiffusion technique involving small probes flush-mounted in the wall was often used to measure local values of wall shear rate (Hanratty and Campbell, 1983). The probe active surface area works as a small electrode where a fast electrochemical reaction takes place. The reduction of ferricyanide ions on a platinum cathode is the most popular electrochemical reaction used for such flow diagnostics:

$$\mathrm{Fe(CN)}_6^{3-} + \mathrm{e}^- \rightarrow \mathrm{Fe(CN)}_6^{4-}. \tag{2}$$

This method consists in measuring the current under diffusional limiting conditions in such a way that the reaction rate is diffusion-controlled through the mass boundary layer, δ_d, and that the ionic migration can be neglected due to the presence of a supporting electrolyte. The measured intensity increases with the applied voltage between the anode and the cathode until it reaches a constant value, $\overline{I}_{\mathrm{lim}}$, corresponding to the limiting diffusion conditions. The mass transfer coefficient, *k*, can then be calculated by

$$k = \overline{I_{\mathrm{lim}}} / v_e \Im A c_0, \tag{3}$$

where v_e is the number of electrons involved in the redox reaction, $\Im$ is the Faraday's constant, *A* is the surface area of the microelectrode and c_0 is the bulk concentration of the reacting species.

The mean measured limiting current is controlled by convective diffusion and the well-known Lévêque formula can be applied to determine the mean wall shear rate, $\bar{s}$. Reiss and Hanratty (1963) solved the stationary equation for a circular microelectrode and found the following relationship:

$$\overline{I}_{\mathrm{lim}} = 0.677 v_e \Im c_0 d_e^{5/3} D^{2/3} \bar{s}^{1/3}, \tag{4}$$

where d_e is the diameter of the circular electrode, and *D* is the diffusion coefficient of the active species in the solution.

The instantaneous values of wall shear rate, $s(t)$, can be directly related to the measured values of the limiting diffusion current only if the assumption of low flow fluctuations is fulfilled. Under highly unsteady flow conditions, the frequency response of electrodiffusion probes must be taken into account. The correction with respect to probe dynamic behaviour can be done using the

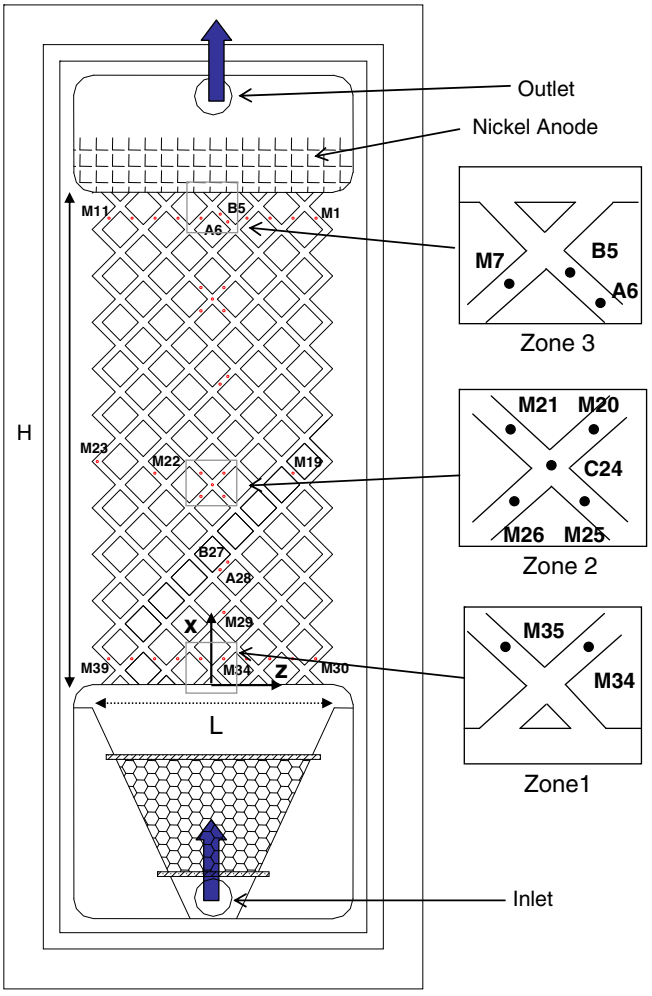

Fig. 2. Scheme of the location of the electrochemical microsensors inside the experimental cell.

corrected solution of Sobolik et al. (1987). These authors solved the mass balance equation assuming that the concentration field is a similar function of three variables:

$$C(x,y,t) = c_0 f(\eta), \tag{5}$$

$$\eta = y f(t)^{1/3}/\delta_d(x), \tag{6}$$

where $f(t)$ is a general time function which takes into account the time shifting of the wall shear rate. The resolution of the diffusion–convection equation in the whole mass boundary layer leads to a general expression of the time history of the wall shear rate, $s(t)$:

$$s(t) = s_q(t) + \frac{2}{3} t_0 \left(\frac{\partial s_q}{\partial t}\right), \tag{7}$$

where s_q is the quasi-steady interpretation solution of the measured current obtained from Eq. (4), given by

$$s_q(t) = 3.22(\nu_e \Im c_0)^{-3} D^{-2} d_e^{-5} I_{\lim}^3(t) \tag{8}$$

and t_0, the characteristic time of the probe defined as a dynamic behaviour parameter of the electrodiffusion probe:

$$t_0(t) = 0.426 d_e^{2/3} D^{-1/3} s_q(t). \tag{9}$$

This relationship was used by several authors in different flow configurations (Tihon et al., 1995; Tihon et al., 2003) who found it relevant at unsteady flow conditions, even by comparison with inverse method (Rehimi et al., 2006).

To characterize the wall turbulence properties, the dimensionless autocorrelation of fluctuating velocity gradient can then be calculated:

$$R_{ss}^* = \frac{R_{ss}}{R_{ss}(0)}. \tag{10}$$

With

$$R_{ss}(t, \mathrm{d}t) = \frac{s'(t)s'(t+\mathrm{d}t)}{\sqrt{s'(t)^2}\sqrt{s'(t+\mathrm{d}t)^2}} \tag{11}$$

and

$$s(t) = \bar{s} + s'(t). \tag{12}$$

Calculation of the autocorrelation provides information regarding the Taylor microscale, λ, and the integral length scale, Λ, by supposing the Taylor hypothesis, which is defined by

$$\lambda = \tau_\lambda \overline{U} \text{ with } R_{ss}^*(t = \tau_\lambda \to 0). \tag{13}$$

Performing a Taylor series expansion of the autocorrelation $R_{ss}^*(t)$, the osculating parabola thus obtained is supposed to yield the derivative covariance:

$$R_{ss}^*(t = \tau_\lambda) = 1 - \frac{t^2}{\tau_\lambda^2}. \tag{14}$$

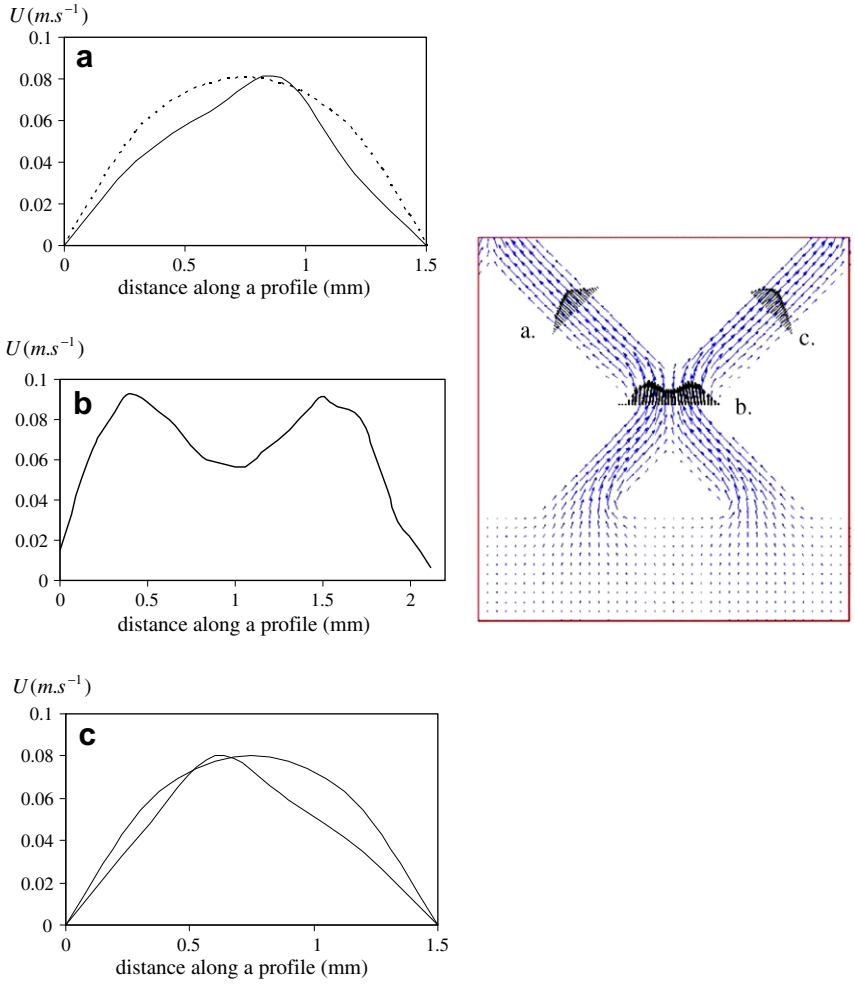

Fig. 3. Velocity profiles and mean flow fields in zone 1 at the inlet for $Re = 144$ (experiments: solid line; analytical solution: dotted line).

The integral scale is given by

$$\Lambda = \overline{U} \int_0^{\infty} R^*_{ss}(t)\,\mathrm{d}t. \tag{15}$$

Integral length scales estimate the size of the largest turbulent eddies and can also be defined as the size of the large energy containing eddies, i.e. eddies containing most of the turbulent kinetic energy. Taylor microscale is a measurement of the dimension of eddies which transfer the kinetic energy at the scale of dissipation where the viscous phenomena predominate. The Taylor microscales represent the small scale motion which are of significant interest in term of molecular mixing or micromixing.

2.4. Electrochemical cell

A home-built electrodiffusion analyser was used to set the polarization voltage to the microelectrodes, to convert the measured currents into voltages and to amplify the resulting signals. A PC computer controlled the analyser operation and data recording. Data records (ranging from 30,000 to 80,000 samples, depending on the Reynolds number value) from eight current signals were provided at a sampling frequency ranging from 3 kHz to 8 kHz.

Thirty-nine circular microelectrodes, made from a platinum wire 0.25 mm in diameter, working as cathodes, were flush-mounted in the flow cell shown in Fig. 2.

The anode was made of a nickel grid located at the cell outlet. The microelectrodes are numbered from 1 to 39 from right to left and from top to bottom. All the microelectrodes were calibrated and the diffusion coefficient was measured at room temperature condition. Huchet et al. (2007) described in details the electrochemical method and the experimental conditions.

Different locations were chosen, respectively: in the middle length of minichannels (M), just after (A) or just before (B) a crossing or in a crossing centre (C). A dimensionless parameter was used to locate each probe in the network: the axial direction was represented by X/H and the lateral one by $l/(L/2)$. The experiments are performed for Re ranging from 15 to 3500.

3. PIV results

3.1. Mean velocity fields

The results of mean flow fields are presented in Fig. 3 at low Reynolds number ($Re = 144$) and in Fig. 4 at a higher Re value ($Re = 1270$).

For $Re = 144$, no instability and no significant detachment appear after the crossing channels. Three velocity profiles are plotted, one of them is located at the crossing (Fig. 3b) and is characterized by two peaks corresponding to the laminar velocity profile of each incoming channel. The velocity increases on both sides of the

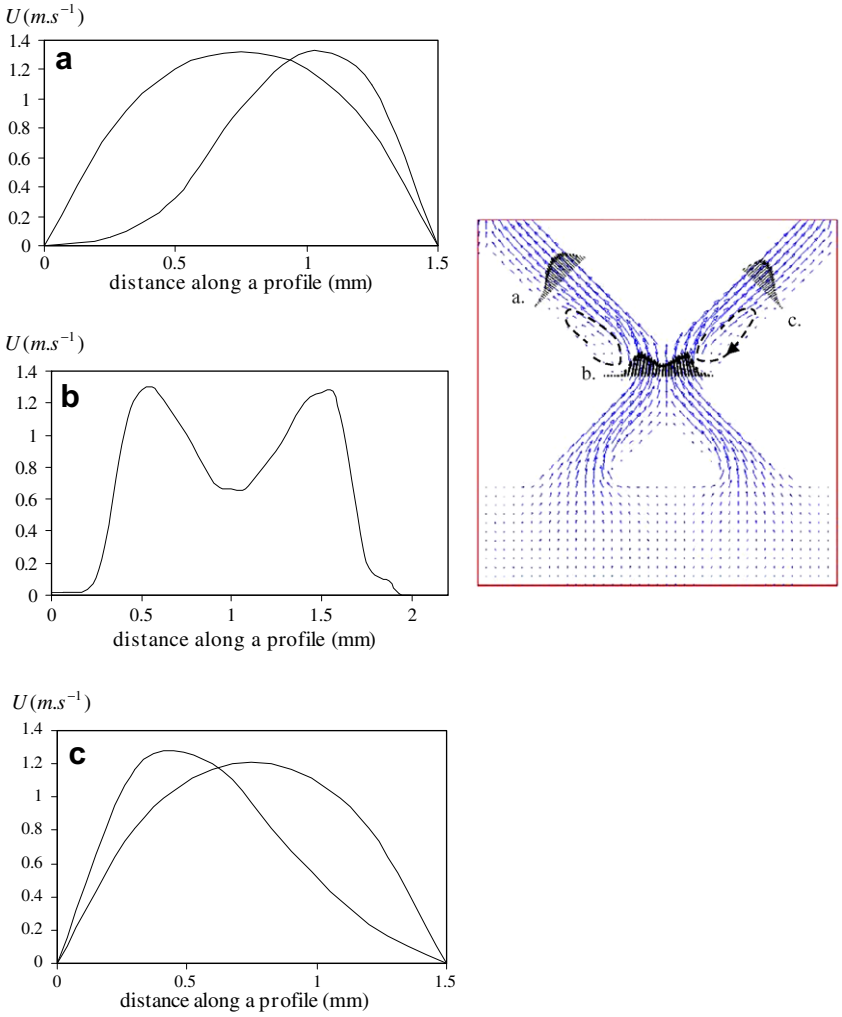

Fig. 4. Velocity profiles and mean flow fields in zone 1 at the inlet for $Re = 1270$ (experiments: solid line; analytical solution: dotted line).

crossing centre and depicts the symmetrical distribution of the flow in the two outlet branches. The mean velocity at the crossing junction is found 1.7 times higher than in the outlet branches (Fig. 3a and c). Normally, the ratio between the velocity at the crossing section and the incoming channel velocity should be $\sqrt{2}$. The lack of resolution in the near wall region tends to overestimate the experimental value. The velocity profiles in the outlet parts are compared with the analytical solution of Natarajan and Lakshmanan (1970) for rectangular channel in fully developed laminar regime, indicating a developing flow at this location in the experimental cell.

For Re = 1270 (Fig. 4), and as previously observed, the velocity decreases in the crossing centre (Fig. 4b). A large recirculation zone is observed on the opposite side of the rear location of the crossing and is associated to a preferential flow which presents more important momentum transfer at this location. The recirculation extends over half of the length between two successive crossings and covers half of its width. The velocity fields are quite similar in each channel after the crossing and the flow structure is non-established after the impact of the two incident streams in comparison to the parabolic profile obtained in fully developed laminar flow (Figs. 4a and c).

3.2. Turbulence intensity fields

For the same Reynolds number, the turbulence intensity fields are presented in Fig. 5 at different levels between the inlet and the outlet of the network of crossing minichannels. Close to the inlet (zone 1), only a small part of the channel emphasizes by a high value of turbulence intensity, reaching 50%. In the middle of the network (zone 2), the disturbed zone grows and spreads over the whole channel between two crossings. This disturbed zone, generated by the presence of the recirculation zone as mentioned in the previous section, persists from the inlet to the outlet (zone 3). At the opposite side, the turbulence intensity at the middle of the channel increases from 10–15% (zone 1) to 25–30% (zones 2 and 3). The crossing junction area is characterized by the reduction of the flow section; it exhibits lower values of turbulent intensities. This zone contributes to damp the flow fluctuations making the heterogeneous spatial flow character in the network. The same characteristics concerning the flow fluctuations in the near wall region have been observed by Huchet et al. (2007). The turbulent intensities decrease is correlated to the disappearance of the recirculation zone at the crossing section.

4. Wall turbulence properties

The limitation of the spatial and temporal resolution in the frame of our PIV measurements in the near wall location justifies the set-up of the electrochemical method which allows the measurement of the instantaneous wall shear rate at the microelectrode location. Moreover, the high acquisition frequencies allow the recognition of the small structures of wall turbulence (Lagraa et al., 2004) and also to identify intermittent properties of a turbulent flow (Adolphe et al., 2007).

4.1. Analysis of wall flow structure at different positions

In Figs. 6–10, the autocorrelation curve of the wall shear rate signals is plotted as a function of time at several locations between the inlet and the outlet of the network corresponding to the position of the microelectrodes in the minichannels. It shows a large

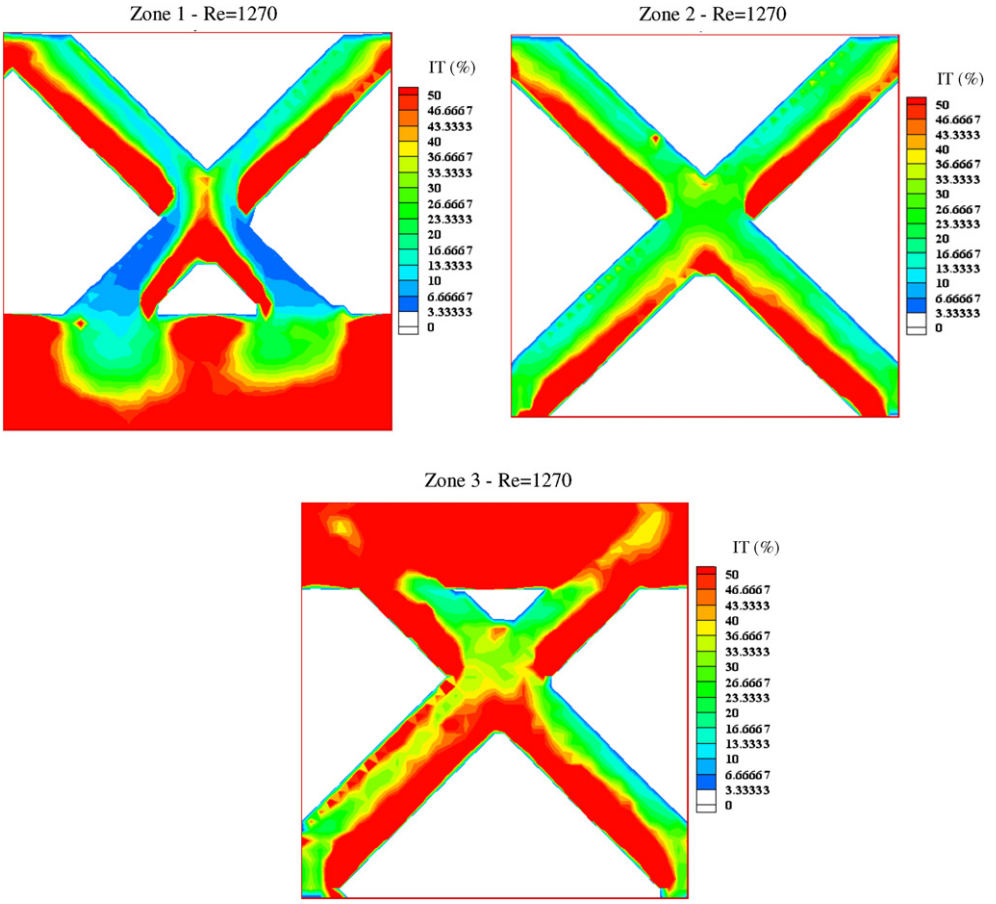

Fig. 5. Turbulence fields in zones 1, 2 and 3 for Re = 1270.

range of characteristic times corresponding to the convective time of the structures in the near location of the probes. Thus, the turbulence macroscales and microscales were calculated according to Eqs. (15) and (14), for $Re = 2950$ by using the Taylor hypothesis.

The sizes of the integral length scale, Λ, and the Taylor microscales, λ, are gathered in Table 1 according to their locations.

- Axial evolution.

The evolution between $x/H = 0.05$ and $x/H = 0.95$ at three locations (M34, M15 and M4) in the axial direction ($0.088 < z/(L/2) < 0.279$) is quite constant. The sizes of the Taylor microscale is equal to 0.74 mm and the sizes of the larger eddies is ranged between 0.97 mm and 1.73 mm which are of the same order of magnitude than the characteristic length of a square minichannel equal to 1.5 mm in side.

- Lateral evolution.

Regarding to the lateral evolution between $z/(L/2) = -0.959$ and $z/(L/2) = 0.733$ at $x/H \approx 0.4$, the results are scattered according to the position in the network. For M25 and M21 position, the sizes of the micro and macroscale respectively equal in average to 0.87 mm and 1.5 mm confirm the previous positions given that their location corresponding to the middle of the network ($z/L/2 \approx 0$) and both to the middle of a channel.

At the lateral positions of the network (M19 and M23) larger integral scales, respectively equal to 3.28 mm and 6.54 mm are observed.

It corresponds to the length of a minichannel between two successive crossings equal to 5.5 mm involving that the shape of these larger vortices are spread out in the longitudinal direction and convected on average along the streamwise direction by the flow. At M23, the correlation coefficient (Fig. 7a) presents a very restricted zone with a parabolic behaviour and can not satisfy the calculation of the Taylor microscale.

- At the channels crossings ("A, B, C" probes).

In the crossing location (Fig. 8), at a smaller scale, the Taylor microscales are of the same order of magnitude at the crossing junction and before the crossing ($\overline{\lambda} \approx 0.88$ mm) excepted for B5 position (Fig. 9) where a lower value is reported. This value is assumed to be due to the outlet effects which especially disturb the flow at this location. This particularity was already mentioned in Section 3.2 where the turbulent intensity field at the outlet is not representative of the remaining of the crossing flow inside the network.

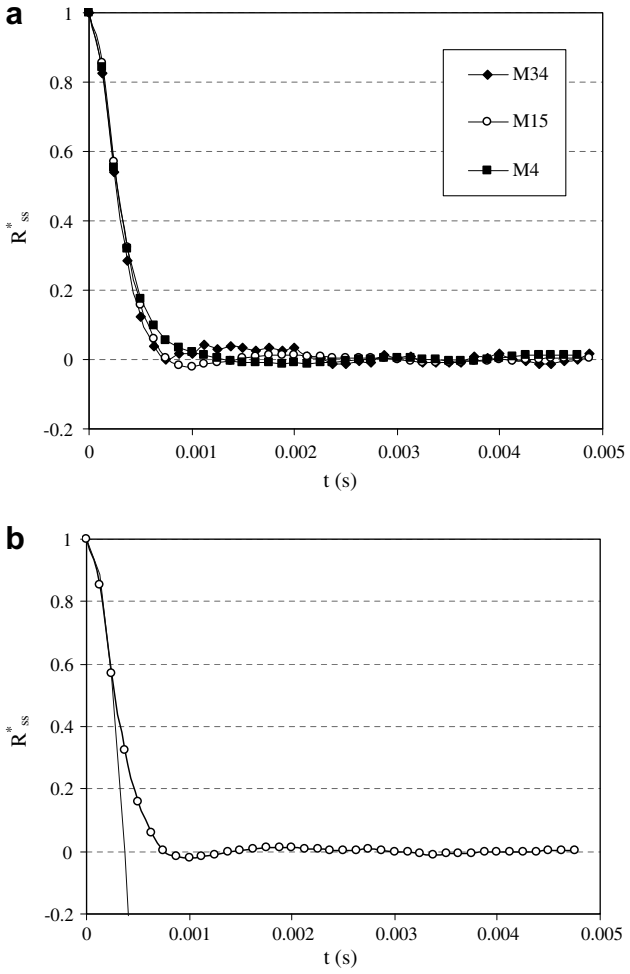

Fig. 6. (a) Dimensionless autocorrelation of the wall shear rate at the middle positions in the axial direction along the network for $Re = 2950$. (b) Autocorrelation function (solid line and open circle) at M15 location and osculating parabola (dotted line) function ($\tau_\lambda = 0.00044$ s).

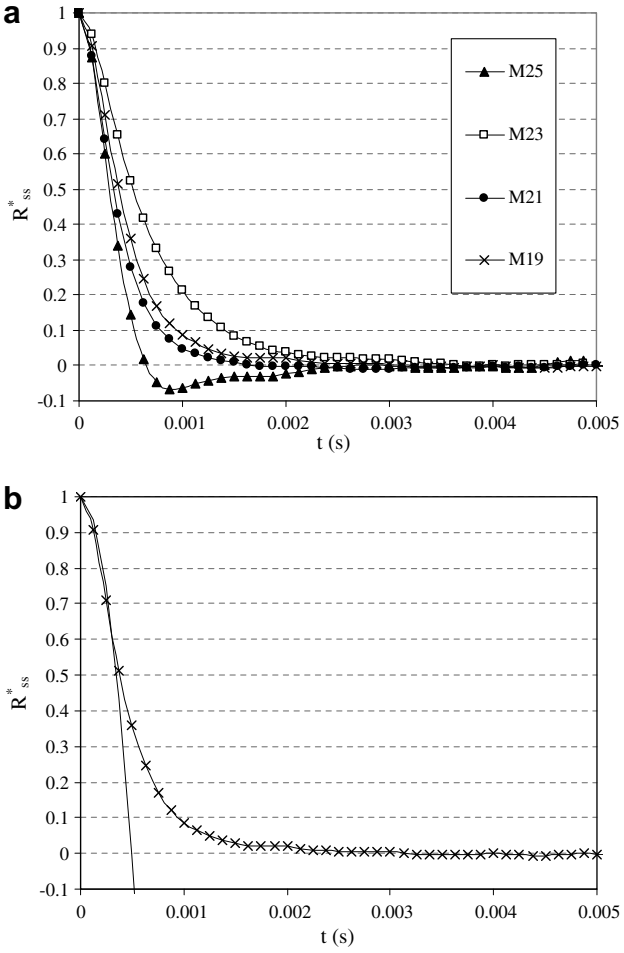

Fig. 7. (a) Dimensionless autocorrelation of the wall shear rate for different positions in the radial direction at $X/H \approx 0.4$ for $Re = 2950$. (b) Autocorrelation function (solid line and crossing) at M19 location and osculating parabola (solid line) function ($\tau_\lambda = 0.0005$ s).

For microelectrodes located after the crossing (A) (Fig. 10), the low values of Taylor microscales ($\overline{\lambda} \approx 0.59$ mm) are maintained due to the recirculation zone observed by PIV.

The sizes of the macroscales at "A" and "C" positions equal in average to 1.5 mm are lower than at position "B". In the first two locations, the sizes are controlled by the junction at the crossing involving the reduction of the flow section, while "A" position presents smaller turbulent scales induced by the recirculation zone. The mean size of the macroscales ($\overline{\Lambda} \approx 2.77$ mm) found at the "B" position corresponds to the length between the crossing and the recirculation zone.

Finally, results regarding characteristic length scales of the turbulence (integral scales and Taylor microscales) show very different trends according to the geometry. Thus, from the PIV and electrochemical measurements, a general pattern describing the different scales inside a crossing of two minichannels transposable to the whole network of crossing minichannels in the constant fluctuations flow regime is proposed in Fig. 11. The integral scales are clearly dependent on the position in the network and particularly influenced by elbows and crossings.

In the present study, the confined geometry addicted by the crossing effects induces anisotropic spatial scales characteristics depending on the position in the channel and in the whole network.

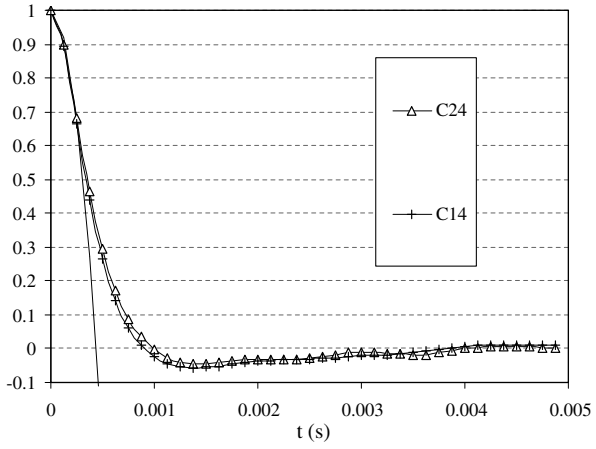

Fig. 8. Dimensionless autocorrelation of the wall shear rate at crossing location and osculating parabola (dotted line) function ($\tau_\lambda = 0.00044$ s).

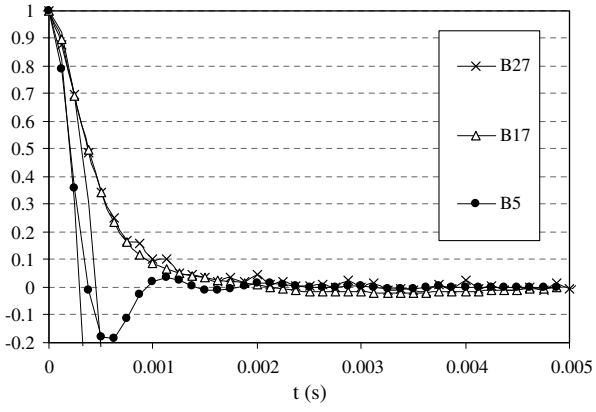

Fig. 9. Dimensionless autocorrelation of the wall shear rate at "B" location and osculating parabola (solid line and dotted line) function ($\tau_\lambda = 0.0003$ s , $\tau_\lambda = 0.00045$ s).

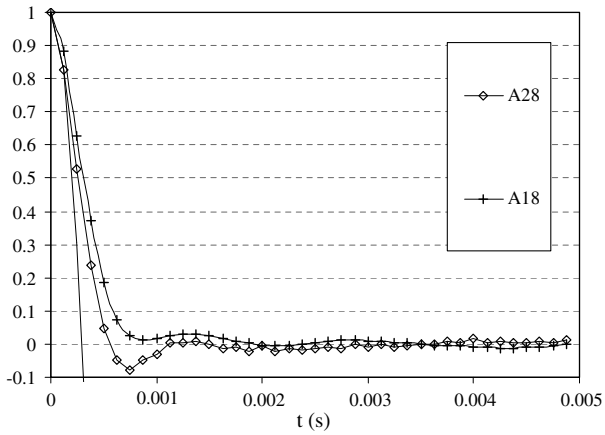

Fig. 10. Dimensionless autocorrelation of the wall shear rate at "A" location and osculating parabola (dotted line) function ($\tau_\lambda = 0.0003$ s).

Table 1
Comparison of the macroscales, Λ, and the Taylor microscales, λ, at different locations in the network for $Re = 2950$

	Probes	X/H	$l/(L/2)$	τ_λ (ms)	λ (mm)	τ_Λ (ms)	Λ (mm)
Lateral evolution	M25	0.39	0.088	0.44	0.87	0.47	0.92
	M23	0.46	−0.959			3.32	6.54
	M21	0.43	−0.102	0.44	0.87	0.98	1.93
	M19	0.43	0.733	0.5	0.98	1.67	3.28
Axial evolution	M34	0.05	0.088	0.375	0.74	0.88	1.73
	M15	0.76	0.088	0.375	0.74	0.49	0.97
	M4	0.95	0.279	0.375	0.74	0.62	1.22
Crossing junction	C24	0.41	−0.008	0.44	0.87	0.81	1.59
	C14	0.79	−0.008	0.44	0.87	0.72	1.42
Before a crossing	B27	0.25	0.12	0.45	0.89	1.46	2.87
	B17	0.63	0.12	0.45	0.89	1.35	2.66
	B5	0.96	0.057	0.3	0.59		
After a crossing	A28	0.23	0.057	0.3	0.59	0.35	0.69
	A18	0.61	0.057	0.3	0.59	0.78	1.54

4.2. Statistical approach

In this section statistics calculation is implemented and analysed in order to qualify the hydrodynamics in term of degree of intermittency or anisotropy.

Experimental and numerical data dealing with intermittent turbulent flow are often characterized by statistical properties which are really different than in homogeneous and isotropic turbulence (Xu et al., 2006; Portelli et al., 2003). Most of the works concerning the study of the turbulent boundary layer has shown that this region is characterized by the presence of ejection of coherent structures called "burst phenomena". These near wall characteristics are linked by the presence of high velocity gradient and the measurements of the fluctuating quantities such as concentration or temperature are characterized by strong and rare fluctuations. In particular, the probability density function is deformed and the dimensionless fourth order moment, i.e. the flatness factor, F, is very different from the value 3 calculated in the case of Gaussian fluctuations. Moreover, the dimensionless third order moment, i.e. the skewness factor, S_k, can significantly increase above zero, which reveals intermittent and strong fluctuations. In the present work, we studied the small scales statistics issued of the electrochemical signals which are linked to the instantaneous limiting diffusion current. The fluctuations of the current correspond to the fluctuations of the concentration of the electrochemical species in the diffusion boundary layer.

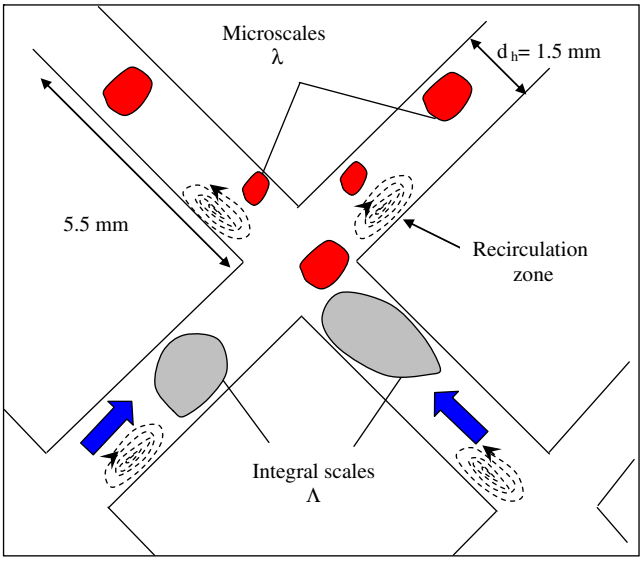

Fig. 11. Multi-scales hydrodynamic pattern in the near wall region.

Time-evolution of the fluctuating value of the wall shear rate measured at the location M15 is given in Fig. 12a for $Re = 2950$. The temporal shifting around the mean value is the first criteria of the intermittency characteristics. More important positives fluctuations are noticed. The normalized histogram of the data (Fig. 12b) is compared with a Gaussian distribution and confirms the intermittency of the electrochemical signals characterized by asymmetrical and non-Gaussian distribution of the fluctuations corresponding to a flatness factor of 8.3. Moreover, the skewness factor, S_k, which reveals the intensity of the fluctuations when its value is greater than 0, reaches 1.55 at this location.

For the purpose of our work, flatness and skewness factors are gathered (Fig. 13) for few locations corresponding to the positions of various microelectrodes. The calculation of the statistical properties of the electrochemical current have been performed by Adolphe et al. (2007) for transitional and turbulent straight channel flow which have described three different regimes such as

- at $Re < 2000$, in the laminar regime, the skewness values are $S_k \approx 0.3$ and flatness values are $F \approx 1.5$ revealing a range of fluctuations containing very low frequencies,
- for $2000 < Re < 4000$, in the transient regime, the skewness factor is $S_k \approx 0.75$, which reveals the existence of strong and rare positive fluctuations associated with burst phenomena,
- in the turbulent regime ($Re > 10{,}000$), $S_k \approx 0$ and $F \approx 3$.

For most of the positions, the variation of F and S_k according to the Reynolds number are really different than in the straight channel configuration. Flatness factor (Fig 13a) varies between 3 and 11 until $Re \approx 1800$. From $Re \approx 1800$ to $Re \approx 2800$, the values decrease until to reach a constant value shifting between 5 and 8. The values of the skewness factor (Fig. 13b) are ranged between 1 and 2 from the constant fluctuation flow regime ($Re > 1000$). Thus, these statistical properties confirm a transient flow regime in the network of crossing minichannels. The transient flow regime is expanded

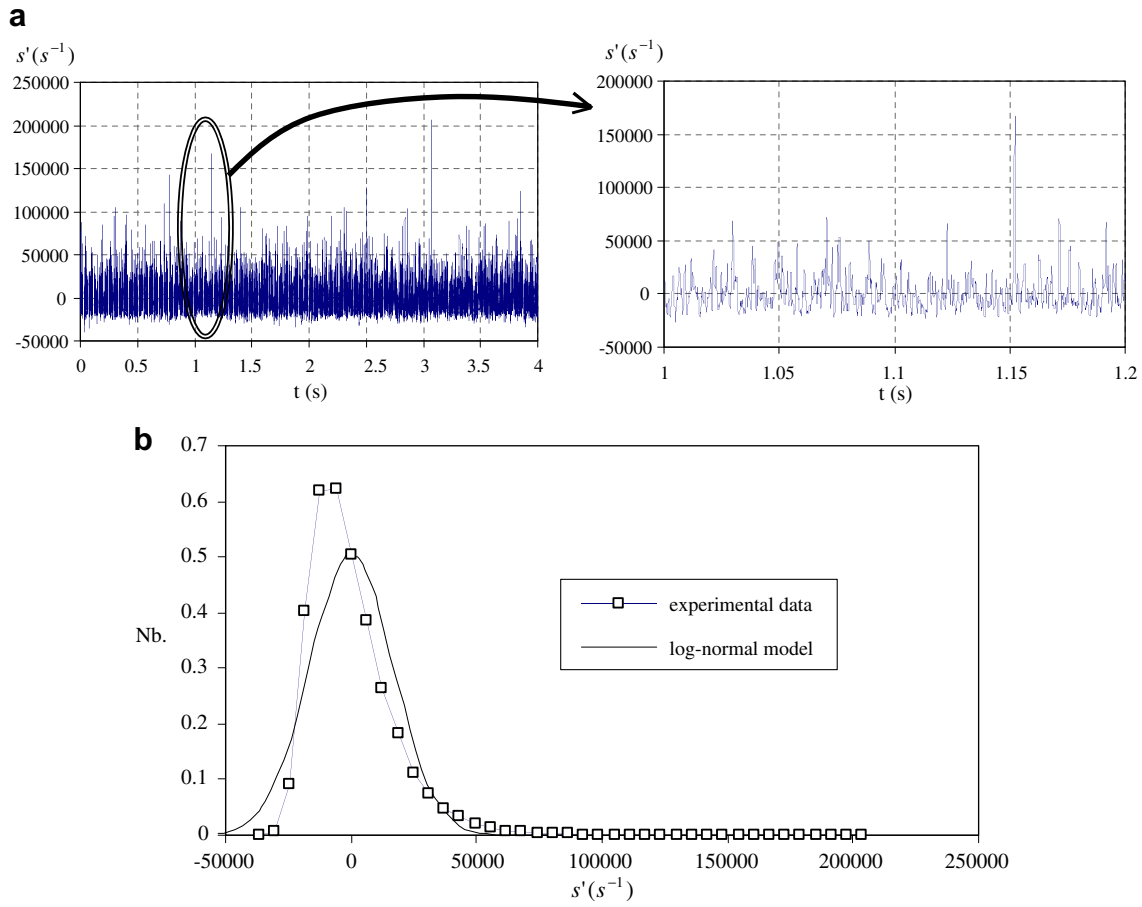

Fig. 12. (a) Time-variation of the fluctuating wall shear rate at the location M15 for $Re = 2950$. (b) Normalised distribution of the fluctuating wall shear rate at the location M15 for $Re = 2950$ and comparison with a log-normal model.

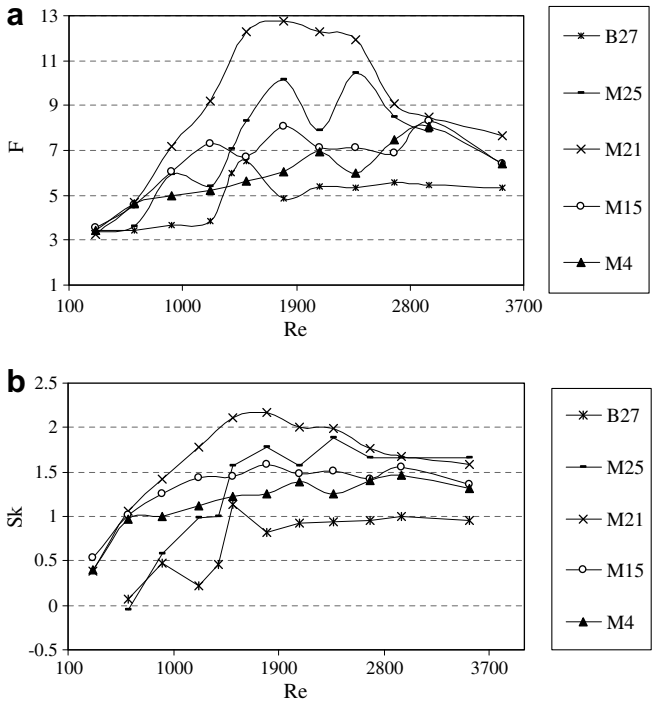

Fig. 13. (a) Evolution of the flatness factor with the Reynolds number. (b) Evolution of the skewness factor with the Reynolds number.

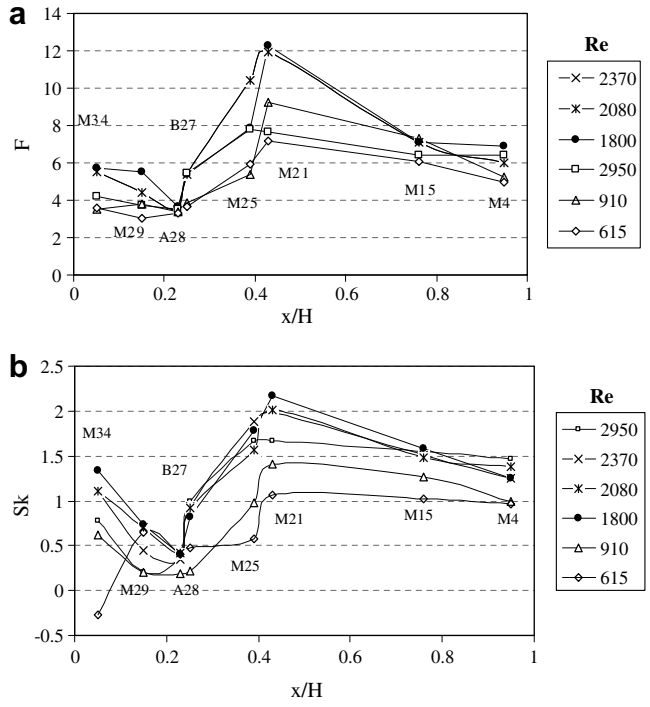

Fig. 14. (a) Evolution of the flatness factor in the network of crossing minichannels for various Reynolds numbers. (b) Evolution of the skewness factor in the network of crossing minichannels for various Reynolds numbers.

above a Reynolds number equal to 1000 in spite of a constant fluctuation rate of the wall shear rate calculated by spectral analysis (Huchet et al. (2007)). Moreover, the fluctuations are noticeably stronger and the intermittent level is larger than in the case of a straight channel in transient regime.

In addition to the Reynolds number on the intermittency level, one can also notice about the influence of the axial location (Fig. 14). The locations corresponding to the microelectrodes M29, A28 and B27 are characterized by lower values of the flatness and skewness factors. This zone ($0 < x/H < 0.3$) was found (Huchet et al., 2007) as being the establishing length of the flow inside the network of crossing minichannels. The high values found at M34 are attributed to some inlet effects already mentioned in the PIV discussion in Section 3.2. At $x/H \approx 0.4$, the intermittency level rises and is found as be maximum at this location in the network whatever the Reynolds number considered. Beyond $x/H \approx 0.4$, the intermittency level is stable whatever the Reynolds number until the outlet ($x/H \approx 0.95$).

The statistical properties of the fluctuating values of the wall shear rate provide information regarding the intermittency characteristics of the flow in the near wall region at several locations inside the network of crossing minichannels. This statistical analysis allows us to verify the previous results discussed in Section 4.1 about the anisotropic scales observed inside a confined flow. Nevertheless, in the present case, it seems that the crossings could be also responsible of the intermittency by the decrease of the fluctuation rate of the wall shear rate at the junction.

5. Conclusion

PIV and electrochemical measurements have been carried out inside a network of crossing minichannels in order to analyse the characteristic scales of the flow.

PIV velocity data emphasize the developing behaviour of the flow between two successive crossings in the whole network.

The inhomogeneous characteristics of the flow are confirmed by using wall electrochemical microsensors at different locations in the network. The wall turbulence eddies are studied by direct high frequency measurements of the wall shear rate. It shows unusually small scales characteristics: integral scales and Taylor microscales are relatively scattered and tend to be dependent on the cell geometry. Higher sizes of the integral scales are found in the lateral part than in the central one of the network. The contribution of the crossings as regards the size of the mixing eddies is less important in the lateral zone ($-0.73 > z/L/2 > 0.96$) than in the axial zone ($-0.3 < z/L/2 < 0.3$). The Taylor microscales are controlled by the confinement effects which induce a scattered spatial distribution between two successive crossings.

This spatial heterogeneous distribution of the small scales is added to a temporal intermittency analysed by means of the statistical properties of the fluctuating wall shear rate quantities. We generally noted that the flatness and the skewness factors are respectively greater than 5 and greater than 1. Thus, the intermittency level is clearly larger than in the case of a straight channel in transient regime. The constant regime fluctuation defined from $Re \approx 1000$ corresponds to a high level of intermittency which starts at $x/H \approx 0.3$, is maximum at $x/H \approx 0.4$ then reaches a stabilization beyond $x/H \approx 0.4$.

Finally, a pattern of the small scales of flow has been proposed in the constant fluctuation regime, taking into account both PIV and wall shear stress data.

One main conclusion is that miniaturized systems exhibits the best conditions to transfer scalar quantities (i.e. concentration, temperature, etc.). In this work, it results anisotropic flow condition characterized by transient regime with intermittency phenomena involving vortices elongated in the streamwise direction. Improvement of electrochemical apparatus (size of the probes, data acquisition) coupled with μPIV measurements should give

fin investigation of the confined flow for which wall–flow interactions predominate. It is crucial to control the dynamic of the unsteady streaks in the near wall region and so the enhancement of the mass or heat transfer inside microdevice.

References

Adolphe, X., Danaila, L., Martemianov, S., 2007. On the small-scale statistics of turbulent mixing in electrochemical systems. J. Electroanal. Chem. 600, 119–130.

Bothe, D., Stemich, C., Warnecke, H.J., 2006. Fluid mixing in a T-shaped micro-mixer. Chem. Eng. Sci. 61, 2950–2958.

Brandner, J.J., Anurjew, E., Bohnn, L., Hansjosten, E., Henning, T., Schygulla, U., Wenka, A., Shubert, K., 2006. Concepts and realization of microstructure heat exchangers for enhanced heat transfer. Exp. Therm. Fluid Sci. 30, 801–809.

Commenge, J.M., Falk, L., Corriou, J.P., Matlosz, M., 2004. Intensification des procédés par microstructuration. C.R. Phys. 5, 597–608.

Deslouis, C., Gil, O., Tribollet, B., 1990. Frequency response of electrochemical sensors to hydrodynamic fluctuations. J. Fluid Mech. 215, 85–100.

Gavrilidis, A., Angeli, P., Cao, E., Yeong, K.K., Wan, Y.S.S., 2002. Technology and applications of microengineered reactors. Trans. IChemE A 80, 3–30.

Hanratty, T.J., Campbell, J.A., 1983. Measurement of wall shear stress. In: Goldstein, J.R.. Fluid Mechanics Measurements. Hemisphere, Washington, p. 559.

Hansen, C., Quake, S.R., 2003. Microfluidics in structural biology: smaller, faster...better. Curr. Opin. Struct. Biol. 13, 538–544.

Huchet, F., Comiti, J., Tihon, J., Montillet, A., Legentilhomme, P., 2007. Electrodiffusion diagnostics of the flow and mass transfer inside a network of crossing minichannels. J. Appl. Electrochem. 37, 49–55.

Kockmann, N., Kiefer, T., Engler, M., Woias, P., 2006. Convective mixing and chemical reactions in microchannels with high flow rates. Sensors Actuat. B 117, 495–508.

Lagraa, B., Labraga, L., Mazouz, A., 2004. Characterization of low-speed streaks in the near-wall region of a turbulent boundary layer. Eur. J. Fluid Mech. 23, 587–599.

Lebouché, M., 1968. Contribution à l'étude des mouvements turbulents par la méthode polarographique. Thèse d'Etat, Nancy.

Legrand, J., Aouabed, H., Legentilhomme, P., Lefèvre, G., 1997. Use of electrochemical sensors for the determination of wall turbulence characteristics in annular swirling decaying flows. Exp. Therm. Fluid Sci. 15, 125–136.

Li, H., Olsen, M., 2006. Examination of large-scale structures in turbulent microchannel flow. Exp. Fluids 40, 733–743.

Natarajan, N.M., Lakshmanan, S.M., 1970. Analytical method for the determination of the pressure drop in rectangular ducts. Indian Chem. Eng. 12, 68–69.

Natrajan, V.K., Christensen, K.T., 2007. Microscopic particle image velocimetry measurements of transition to turbulence in microscale capillaries. Exp. Fluids 43, 1–16.

Natrajan, V.K., Yamaguchi, E., Christensen, K.T., 2007. Statistical and structural similarities between micro- and macroscale wall turbulence. Microfluid. Nanofluid. 3, 8–100.

Portelli, B., Holdsworth, P.C.W., Pinton, J.F., 2003. Intermittency and non-Gaussian fluctuations of the global energy transfer in fully developed turbulence. Phys. Rev. Lett. 90, 104501_1–104501_4.

Rehimi, F., Aloui, F., Ben Nasrallah, S., Doubliez, L., Legrand, J., 2006. Inverse method for electrodiffusional diagnostics of flow. Int. J. Heat Mass Transfer 49, 1242–1254.

Reiss, L.P., Hanratty, T.J., 1963. An experimental study of the unsteady nature of the viscous sublayer. AIChE J. 8, 154–160.

Seguin, D., Montillet, A., Comiti, J., 1998a. Experimental characterization of flow regimes in various porous media – I: limit of laminar flow regime. Chem. Eng. Sci. 53, 3751–3761.

Seguin, D., Montillet, A., Comiti, J., Huet, F., 1998b. Experimental characterization of flow regimes in various porous media II: transition to turbulent regime. Chem. Eng. Sci. 53, 3897–3909.

Sobolik, V., Wein, O., Cermak, K.J., tul=0?>Sobolik et al., 1987. Simultaneous measurement of film thickness and wall shear stress in wavy flow of non-Newtonian liquids. Coll. Czech Chem. Com. 52, 913–928.

Sobolik, V., Tihon, J., Wein, O., Wichterle, J.K., tul=0?>Sobolik et al., 1998. Calibration of electrodiffusion friction probes using a voltage-step transient. J. Appl. Electrochem. 28, 329–335.

Tihon, J., Legrand, J., Aouabed, H., Legentilhomme, P., 1995. Dynamics of electrodiffusion probes in developing annular flows. Exp. Fluids 20, 131–134.

Tihon, J., Tovchigrechko, V., Sobolik, V., Wein, O., 2003. Electrodiffusion of the near-wall reversal in liquid films at the regime of solitary waves. J. Appl. Electrochem. 33, 577–587.

Wu, Z., Nguyen, N.T., 2005. Hydrodynamic focusing in microchannels under consideration of diffusive dispersion: theories and experiments. Sensors Actuat. B 107, 965–974.

Xu, C.X., Li, L., Cui, G.X., Zhang, Z.S., 2006. Multi-scale analysis of near-wall turbulence intermittency. J. Turbulence 7, 1–15.